***Original Research Article***

# Global Thermal instability in the spherical interstellar clouds


## Abstract

Aims :Thermal instability (TI) is a trigger mechanism, which can explain formation of small condensations through some regions of the interstellar clouds. Our goal here is to investigate the conditions for occurrence of TI through the thermally dominated (i.e., gravitationally stable) quasi-static spherical interstellar clouds.

Methodology: We use the perturbation method to investigate the linear regime of instability and finding its growth rate.

Results: Considering spherical perturbations on the quasi-static spherical cloud, instead of a thermal and dynamical equilibrium flat cloud, changes the instability criterion, so that we can conclude that sphericalness can increase the occurrence of TI. The results show that in the spherical clouds, perturbations with shorter wavelengths have more chance to grow via TI (i.e., greater growth rates).


*Keywords: ISM: clouds; stars:formation; ISM: evolution; hydrodynamics*

## 1 Introduction

After the pioneer paper of [1], entitled *thermal instability* (TI), this subject appeared to be an important mechanism to explain formation of density condensations through the interstellar and intergalactic clouds. This mechanism is used to explain a wide range of multiphase phenomena from local intra-galactic situations to large extra-galactic occurrences (e.g., [2-10]).

The most important parameter for occurrence of TI is the net cooling function $\Omega(\rho, T)$. In a local thermal and dynamical equilibrium flat clouds, the isobaric instability criterion is $\Omega_T - (\frac{\rho_0}{T_0})\Omega_\rho < 0$, where $\Omega_\rho \equiv (\partial\Omega/\partial\rho)_T$ and $\Omega_T \equiv (\partial\Omega/\partial T)_\rho$ are evaluated in equilibrium state. Using the flat plane perturbations to investigate local TI can be appropriate in some

interstellar gases, but, many interstellar clouds have a spherical structure. Thus, the flat plane approximation is not completely correct for global TI, and it is better to use spherical perturbations.

For this purpose, in § 2 we consider thermally equilibrium models for quasi-static spherically symmetric clouds. The effect of spherical perturbations are investigated in §3. Section 4 is devoted to summary and conclusions.

## 2 Thermally equilibrium models

In the spherical polar coordinates, the usual hydrodynamic equations for spherically symmetric thermally dominated clouds are

$$\frac{\partial \rho}{\partial t}+\frac{1}{r^2}\frac{\partial}{\partial r}\left(r^2\rho u\right)=0, \tag{2.1}$$

$$\frac{\partial u}{\partial t}+u\frac{\partial u}{\partial r}=-\frac{1}{\rho}\frac{\partial p}{\partial r}-\frac{GM}{r^2}, \tag{2.2}$$

$$\frac{\partial M}{\partial t}+u\frac{\partial M}{\partial r}=0, \quad \frac{\partial M}{\partial r}=4\pi r^2\rho, \tag{2.3}$$

$$\frac{\partial p}{\partial t}+u\frac{\partial p}{\partial r}+\gamma p\frac{1}{r^2}\frac{\partial}{\partial r}\left(r^2u\right)=-\left(\gamma-1\right)\rho\Omega, \tag{2.4}$$

$$p=\frac{k_B}{\mu m_H}\rho T, \tag{2.5}$$

where mass density $\rho$, the enclosed mass $M$, radial flow velocity $u$, thermal gas pressure $p$ and temperature $T$ depend on the radius $r$ and time $t$; $G$ is the gravitational constant, $\gamma$ is the heat capacity ratio, and $k_B$, $\mu$ and $m_H$ are Boltzmann constant, the mean particle weight and the hydrogen mass, respectively. The net cooling function is presented by $\Omega(\rho,T)=\rho^2\Lambda(T)-\rho\Gamma$ where $\Lambda$ and $\Gamma$ are the cooling and heating rates, respectively.

Determination of the net cooling function $\Omega$ for optically thick and/or optically thin interstellar gas is a complex non-local thermodynamic equilibrium radiative transfer problem. For example, [4] used the results of [11] to parameterize the cooling rate for molecular clouds as $\propto (T/10\,\mathrm{K})^{\beta}$ where the parameter $\beta$ and proportional constant are given in the figure 1 of his paper. For heating mechanisms, he considered different heating mechanisms such as heating due to cosmic rays (e.g., [12]), dissipation of magnetic energy via ambipolar diffusion (e.g.,[13]), and so on. As another example, [14] used the data of [15] to approximate an analytic function for cooling rate in the circumgalactic medium as

$$\Lambda(T)=3.9\times10^{26}\times10^{\Theta(\log(T/10^5\,\mathrm{K})}\,\mathrm{erg\,cm^3\,g^{-2}\,s^{-1}}, \tag{2.6}$$

where the exponent is

$$\Theta(x)=0.4x-3+\frac{5.2}{e^{x+0.08}+e^{-1.5(x+0.08)}}. \tag{2.7}$$

For hating rate, they used a constant value $\Gamma=0.06\,\mathrm{erg\,g^{-1}\,s^{-1}}$, which is expected from photoelectric explosion of electrons from dust grains.

In the stationary ($\partial/\partial t = 0$) quasi-static ($u \to 0$) thermally equilibrium state, the net cooling function $\Omega(\rho, T)$ is assumed to be zero at each radius $r$ (i.e., locally thermal balance). This thermal balance (i.e., $\Omega(\rho, T) = 0$) leads to a relation between the temperature $T$ and density $\rho$ at each radius. Here, we use a parametric relation between density and temperature as $T = \rho^{\eta}$, where $\eta$ is a constant parameter. We consider three state-of-the-art models for temperature change according to the density decrease of the cloud: (i) decreasing temperature by $\eta > 0$, (ii) increasing temperature by $\eta > 0$, and constant temperature by $\eta = 0$.

Knowing the relation between temperature and density, equation (2.5) leads us to determine the gradient of pressure as

$$\frac{dp}{dr} = \frac{k_B}{\mu m_H}\left(T + \rho\frac{dT}{d\rho}\right)\frac{d\rho}{dr}, \tag{2.8}$$

so that the stationary ($\partial/\partial t = 0$) quasi-static ($u \to 0$) state of the momentum equation (2.2) becomes

$$\frac{d\rho}{dr} = -\frac{\mu m_H G}{k_B}\frac{M\rho}{r^2\left(T + \rho\frac{dT}{d\rho}\right)}. \tag{2.9}$$

We use the non-dimensional quantities $\tilde{\rho} \equiv \rho/\rho_r$, $\tilde{T} \equiv T/T_r$, $\tilde{r} \equiv r/(\frac{k_B T_r/\mu m_H}{4\pi G\rho_r})^{\frac{1}{2}}$, and $\tilde{M} \equiv M/4\pi(\frac{k_B T_r/\mu m_H}{4\pi G\rho_r})^{\frac{3}{2}}\rho_r$, where $\rho_r$ and $T_r$ are the reference density and temperature, respectively. In this way, the equations (2.3) and (2.9) become

$$\frac{d\tilde{M}}{d\tilde{r}} = \tilde{r}^2\tilde{\rho}, \tag{2.10}$$

$$\frac{d\tilde{\rho}}{d\tilde{r}} = -\frac{\tilde{M}\tilde{\rho}^{1-\eta}}{\tilde{r}^2\tilde{T}(1+\eta)}, \tag{2.11}$$

where the thermal balance relation $\tilde{T} = \tilde{\rho}^{\eta}$ is used. The differential equations (2.10) and (2.11) can be integrated numerically (e.g., with Runge-Kutta method), from the origin $\tilde{r} = 0$ with the boundary conditions $\tilde{\rho}(0) = \tilde{\rho}_c$ and $\tilde{M}(0) = 0$, where $\tilde{\rho}_c$ is the non-dimensional central density. The density profiles of some models with different values of the parameter $\eta$ are depicted in Fig. 1.

# 3 Perturbations in the cloud

The quasi-static spherical interstellar clouds with low density contrast are mainly confined by the external pressure. If the density contrast exceeds a critical value (e.g., Bonnor-Ebert sphere), the cloud will have gravity-dominated configurations, and an arbitrarily small initial perturbation in the structure grows rapidly with time, leading ultimately to collapse. Here, we turn our attention to the gravitationally stable cloud with masses less than the critical value of the Bonnor-Ebert sphere. If perturbations occur in the structure of these clouds, the thermal effects will be important for growth (i.e., thermal instability) or decay (i.e., thermal stability) of them. To investigate this effect, we split each variable into unperturbed and perturbed components; the latter is indicated by subscript '1'. We perform the linear perturbation analysis, with time and radius Fourier expansions, $A_1(r,t) = A_1^d \exp(\omega t + ikr)$,

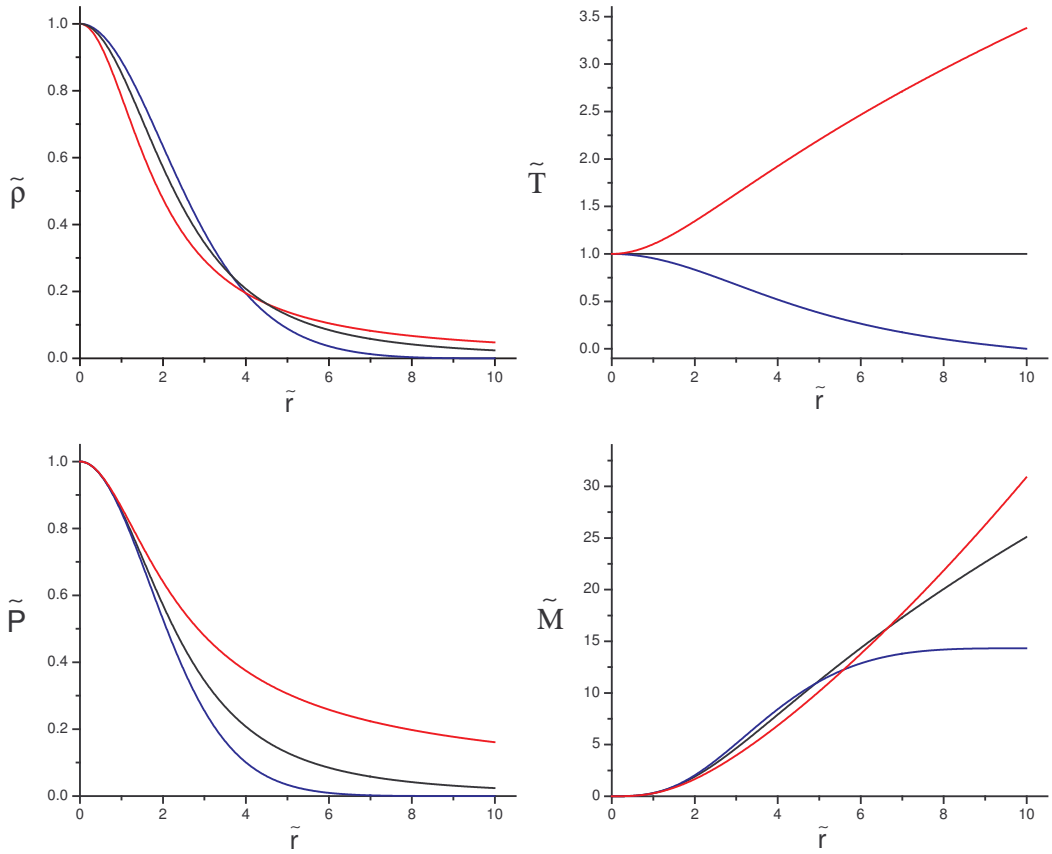


Figure 1: The thermally equilibrium profiles of non-dimensional density, temperature, pressure, and enclosed mass for a quasi-static spherically symmetric interstellar cloud. The solid black curves are for $\eta = 0$, blue curves are for $\eta = 0.4$, and red ones are for $\eta = -0.4$.

on the thermally equilibrium spherically symmetric cloud (in which its variables are denoted by subscript '0'). Time evolution in the non-linear regime is out of scope of this paper. It is of great interest to derive the growth/decay rate, $\Re(\omega)$, for the range of suitable wavelengths, $2\pi/k$, at different radii $r$.

In this way, by using perturbations of the form $\exp(\omega t + ikr)$ for density, radial velocity, enclosed mass, and pressure with amplitudes $\rho_1^d$, $u_1^d$, $M_1^d$, and $p_1^d$, respectively, the equations (2.1)-(2.5) can be linearized by repeated use of the unperturbed equations as follows

$$(\omega)\,\rho_1^d + \left(\rho_0' + \frac{2}{r}\rho_0 + ik\rho_0\right) u_1^d = 0, \tag{3.1}$$

$$\left(-\frac{p_0'}{\rho^2}\right)\rho_1^d + (\omega)\,u_1^d + \left(\frac{G}{r^2}\right) M_1^d + \left(\frac{ik}{\rho_0}\right) p_1^d = 0, \tag{3.2}$$

$$\left(4\pi r^2 \rho_0\right) u_1^d + (\omega)\,M_1^d = 0, \tag{3.3}$$

$$\left[\frac{p_0}{\rho_0}\left(\nu_\rho-\nu_T\right)\right]\rho_1^d+\left(p_0'+\frac{2\gamma}{r}p_0+ik\gamma p_0\right)u_1^d+\left(\omega+\nu_T\right)p_1^d=0, \tag{3.4}$$

where $\nu_T\equiv\frac{\mu m_H(\gamma-1)}{k_B}\left(\frac{\partial\Omega}{\partial T}\right)_\rho$, $\nu_\rho\equiv\frac{\mu m_H(\gamma-1)}{k_B}\frac{\rho_0}{T_0}\left(\frac{\partial\Omega}{\partial\rho}\right)_T$ are angular frequencies of isochoric and isothermal perturbations, respectively [1], and primes denote $\frac{d}{dr}$. Now, if we set the determinant of coefficients matrix equal to zero, we obtain a third degree polynomial characteristic equation as follows

$$\omega^3+C_2\omega^2+C_1\omega+C_0=0, \tag{3.5}$$

where

$$C_0=\left(-4\pi G\rho_0+\frac{p_0'\rho_0'}{\rho_0^2}+\frac{2}{r}\frac{p_0'}{\rho_0}+ik\frac{p_0'}{\rho_0}\right)\nu_T+\left(ik\frac{p_0\rho_0'}{\rho_0^2}+\frac{2ik}{r}\frac{p_0}{\rho_0}-k^2\frac{p_0}{\rho_0}\right)(\nu_\rho-\nu_T), \tag{3.6}$$

$$C_1=-4\pi G\rho_0-\frac{2ik\gamma}{r}\frac{p_0}{\rho_0}+k^2\gamma\frac{p_0}{\rho_0}+\frac{p_0'\rho_0'}{\rho_0^2}+\frac{2}{r}\frac{p_0'}{\rho_0}, \tag{3.7}$$

and $C_2=\nu_T$. These coefficients depend on the wavenumber $k$, and must be evaluated for different radii $r$.

The simplest case is one in which $\eta=0$. Here, we turn our attention to this case, and other models, which depend strictly on the choosing of the net cooling function, will be considered in the subsequent researches. In this case (i.e., $\eta=0$), the density and pressure profiles can be locally (i.e., regions of interest around each radius far from $r\approx0$) approximated as inverse square law, $p_0\,\&\rho_0\propto\frac{1}{r^2}$, and the enclosed mass increases linearly as $M\propto r$. These results can be clearly deduced from Fig. 1. In this way, the coefficients of the characteristic equation (3.5) reduces to

$$C_0=\frac{k^2\bar{c}^2}{\gamma}(\nu_T-\nu_\rho)-ik\frac{2\bar{c}^2\nu_T}{\gamma r}-\frac{2\bar{c}^2\nu_T}{\gamma r^2}, \tag{3.8}$$

$$C_1=k^2\bar{c}^2-ik\frac{2\bar{c}^2}{r}-\frac{2\bar{c}^2}{\gamma r^2}, \tag{3.9}$$

and $C_2=\nu_T$, where $\bar{c}$ is the sound speed. Note that the terms including $1/r$ and $1/r^2$ appear because we used the spherical coordinates to describe the cloud. At very large radii, where the sphericalness is negligible (i.e. $r\to\infty$), these coefficients reduce to the coefficients of the characteristic equation of the well-known pioneered work of [1]. Using non-dimensional quantities

$$y\equiv\frac{\omega}{kc},\quad \sigma_T\equiv\frac{\nu_T}{kc},\quad \sigma_\rho\equiv\frac{\nu_\rho}{kc},\quad \lambda\equiv\frac{1}{kr}, \tag{3.10}$$

the characteristic equation can be written as

$$y^3+\sigma_T y^2+\left(1-2i\lambda-\frac{2\lambda^2}{\gamma}\right)y+\left[\frac{1}{\gamma}\left(\sigma_T-\sigma_\rho\right)-i\frac{2\lambda}{\gamma}\sigma_T-\frac{2\lambda^2}{\gamma}\sigma_T\right]=0. \tag{3.11}$$

Here, we use the Laguerre method (e.g., [16]) to find numerically the roots of the characteristic equation (3.11). The results for instability in the $\sigma_T$-$\sigma_\rho$ plane are shown in the Fig. 2. Note that $\lambda=0$ corresponds to the results of [1], with the usual isobaric and isentropic instability

criterions as $\nu_\rho > \nu_T$, and $\nu_\rho < -(\gamma - 1)\nu_T$, respectively. The results show that increasing of $\lambda$ (i.e., perturbations with longer wavelengthes at each radius $r$) decreases the stability region in the $\sigma_T$-$\sigma_\rho$ plane. The importance of linear TI can be expressed by the growth rate, $\Re(\omega)$, of unstable regions through the $\sigma_T$-$\sigma_\rho$ plane. Finding the roots of (3.11) for different values of $\lambda$ show that $\Re(y/\lambda)$ is a decreasing function of $\lambda$. Thus, at each radial position $r$, perturbations with shorter wavelengths (i.e., smaller $\lambda$) have greater growth rates, which corresponds to more chance for thermally unstable growth.

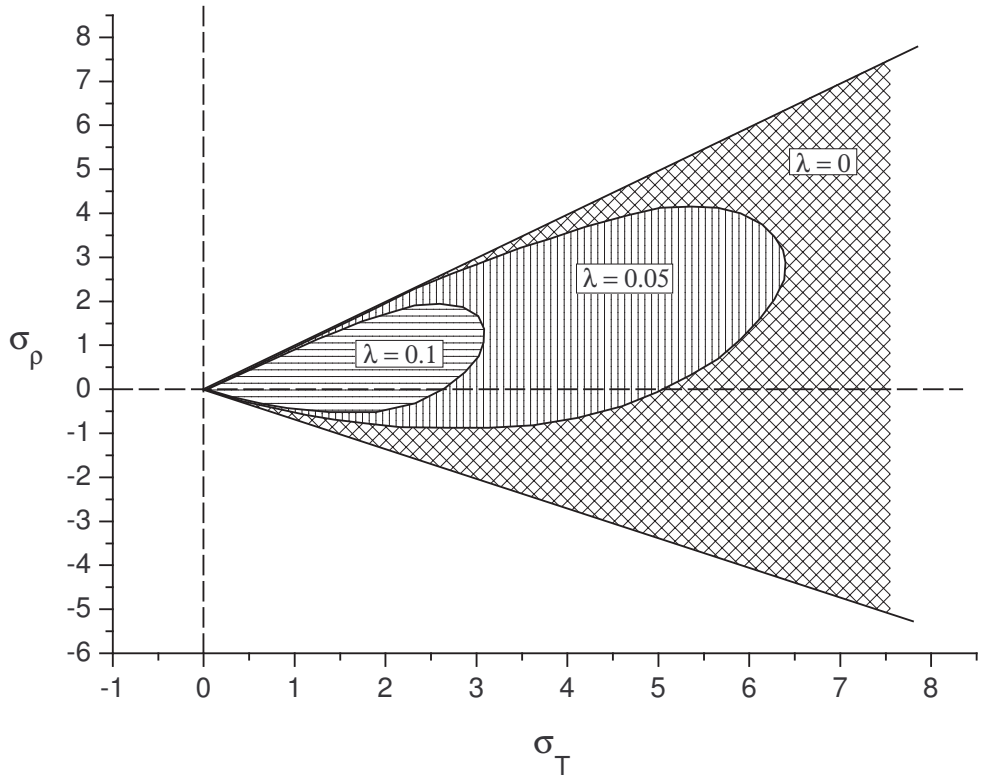


Figure 2: Regions of TI in the $\sigma_T$-$\sigma_\rho$ plane with $\lambda = 0, 0.05$ and $0.1$ for $\gamma = 5/3$. The stable regions are depicted by hatch-patters of diagonal cross for $\lambda = 0$, light vertical lines for $\lambda = 0.05$, and light horizontal lines for $\lambda = 0.1$. In each case of $\lambda$, other regions are thermally unstable.

# 4 Summary and conclusions

TI is an important trigger mechanism that can explains formation of density condensations through some regions of interstellar clouds and circumgalactic medium. In this paper, we turned our attention to a simple model as a spherical cloud, and investigated occurrence

of linear TI through it. First of all, we surveyed thermally equilibrium models of the quasi-static spherically symmetric clouds; the radial profiles of density, temperature, pressure, and enclosed mass are shown in Fig.1. After that, we used the perturbation method to investigate occurrence and growth rates of linear TI through these equilibrium models.

We used a parametric relation between density and temperature as $T = \rho^{\eta}$. We turned our attention to the simplest case in which $\eta = 0$. In this case, the characteristic equation (3.5) reduces to a simple form (3.11), which by ignorance of the sphericalness (i.e., $r \to \infty$ so that $\lambda \to 0$), it reduces to the characteristic equation of the well-known work of Field (1965). The Fig 2 shows the thermally unstable regions in the $\sigma_T$-$\sigma_\rho$ plane; considering the sphericalness of the cores (i.e., greater values of $\lambda$) results in to increase the instability regions in this plane. Also, comparing the real parts of the roots of (3.11) for different values of $\lambda$ demonstrates that at each radius $r$, perturbations with smaller wavelengths become more thermally unstable (i.e., have greater growth rates) than longer ones.

# References

1. Field, G. B. (1965). Thermal Instability. ApJ, 142, 531. DOI: 10.1086/148317

2. Hunter, J. H. (1966). The role of thermal instabilities in star formation. MNRAS, 133, 239. DOI: 10.1093/mnras/133.2.239

3. Fukue, T. & Kamaya, H. (2007). Small Structures via Thermal Instability of Partially Ionized Plasma: I. Condensation Mode. ApJ, 669, 363. DOI: 10.1086/521268

4. Nejad-Asghar, M. (2011). Formation of low-mass condensations in molecular cloud cores via thermal instability. MNRAS, 414, 470. DOI: 10.1111/j.1365-2966.2011.18412.x

5. Choudhury, P. P. & Sharma, P. (2016). Cold gas in cluster cores: global stability analysis and non-linear simulations of thermal instability. MNRAS, 457, 2554. DOI: 10.1093/mnras/stw152

6. Nejad-Asghar, M. (2019). Thermal instability through the outer half of quasi-static spherically symmetric molecular clumps and cores. Ap&SS, 364, 122. DOI: 10.1007/s10509-019-3616-y

7. Dannen, R. C., Proga, D., Waters, T. & Dyda, S. (2020). Clumpy AGN Outflows due to Thermal Instability. ApJ, 893, 34. DOI:10.3847/2041-8213/ab87a5

8. Antolin, P., Martínez-Sykora, J. & Şahin, S, (2022). Thermal Instability-Induced Fundamental Magnetic Field Strands in the Solar Corona. ApJ, 926, 29. DOI: 10.3847/2041-8213/ac51dd

9. Gronkiewicz, D., Różańska, A., Petrucci, P. & Belmont, R, (2023). Thermal instability as a constraint for warm X-ray coronas in active galactic nuclei. A&A, 675,198. DOI: 10.1051/0004-6361/202244410

10. Hermans, J. & Keppens, R. (2024). A spectroscopic investigation of thermal instability for cylindrical equilibria with background flow. A&A, 686, 180. DOI: 10.1051/0004-6361/202348337

11. Neufeld, D. A., Lepp, S. & Melnick, G. J. (1995). Thermal Balance in Dense Molecular Clouds: Radiative Cooling Rates and Emission-Line Luminosities. ApJS, 100, 132. DOI: 10.1086/192211

12. Glassgold, A. E. & Langer, W. D. (1973). Cosmic-Ray Heating and Molecular Cooling

of Dense Clouds. ApJ, 179, 147. DOI: 10.1086/181137

13. Li, P., Myers, A. & McKee, C. F. (2012). Ambipolar Diffusion Heating in Turbulent Systems. ApJ, 760, 33. DOI: 10.1088/0004-637X/760/1/33

14. Wiener, J., Zweibel, E. G. & Ruszkowski, M. (2019). Cosmic ray acceleration of cool clouds in the circumgalactic medium. MNRAS, 489, 205. DOI: 10.1093/mnras/stz2007

15. Wiersma, R. P. C., Schaye, J.& Smith, B. (2009). The effect of photoionization on the cooling rates of enriched, astrophysical plasmas. MNRAS,393, 99. DOI: 10.1111/j.1365-2966.2008.14191.x

16. Press, W. H., Teukolsky, S. A., Vetterling, W. T. & Flannery, B. P. (1992. Numerical recipes in FORTRAN: The art of scientific computing (2th ed.). Cambridge University Press.